



HAL
open science

**Vapor-liquid equilibrium and molecular simulation data
for carbon dioxide (CO₂) +
trans-1,3,3,3-tetrafluoroprop-1-ene (R-1234ze(E))
mixture at temperatures from 283.32 to 353.02 K and
pressures up to 7.6 MPa**

Siyi Wang, Rémi Fauve, Christophe Coquelet, Alain Valtz, Celine Houriez,
Pierre-Arnaud Artola, Elise El Ahmar, Bernard Rousseau, Haitao Hu

► **To cite this version:**

Siyi Wang, Rémi Fauve, Christophe Coquelet, Alain Valtz, Celine Houriez, et al.. Vapor-liquid equilibrium and molecular simulation data for carbon dioxide (CO₂) + trans-1,3,3,3-tetrafluoroprop-1-ene (R-1234ze(E)) mixture at temperatures from 283.32 to 353.02 K and pressures up to 7.6 MPa. International Journal of Refrigeration, 2019, 98, pp.362-371. 10.1016/j.ijrefrig.2018.10.032 . hal-01968756

HAL Id: hal-01968756

<https://hal.science/hal-01968756>

Submitted on 3 Jan 2019

HAL is a multi-disciplinary open access archive for the deposit and dissemination of scientific research documents, whether they are published or not. The documents may come from teaching and research institutions in France or abroad, or from public or private research centers.

L'archive ouverte pluridisciplinaire **HAL**, est destinée au dépôt et à la diffusion de documents scientifiques de niveau recherche, publiés ou non, émanant des établissements d'enseignement et de recherche français ou étrangers, des laboratoires publics ou privés.

Vapor-liquid equilibrium and molecular simulation data for carbon dioxide (CO₂) + trans-1,3,3,3-tetrafluoroprop-1-ene (R-1234ze(E)) mixture at temperatures from 283.32 to 353.02 K and pressures up to 7.6 MPa

Siyi Wang^{1,2}, Rémi Fauve², Christophe Coquelet^{2*}, Alain Valtz², Céline Houriez², Pierre-Arnaud Artola^{3a},
Elise El Ahmar², Bernard Rousseau^{3b} and Haitao Hu¹

1 Institute of Refrigeration and Cryogenics, Shanghai Jiao Tong Univ, 800 Dongchuan Rd, 200240
Shanghai, China

2 Mines ParisTech, PSL Research University, CTP – Centre of Thermodynamics of Processes 35, rue Saint
Honoré 77305 Fontainebleau Cedex France

3a : Laboratoire de Chimie Physique, Université Paris-Sud bâtiment 349, 310 Rue Michel Magat, 91405
Orsay, France

3b : Laboratoire de Chimie Physique, Université Paris-Sud bâtiment 349, UMR 8000 CNRS, 310 Rue
Michel Magat, 91405 Orsay, France

* : Corresponding author : christophe.coquelet@mines-paristech.fr (tel :+33164694962 Fax :+33164694968).

Abstract:

Isothermal Vapor-Liquid Equilibrium (VLE) data for the binary mixture of CO₂ + R-1234ze(E)(trans-1,3,3,3-tetrafluoroprop-1-ene) were measured using a static-analytic method apparatus at seven temperatures between 283.32 and 353.02 K and pressures up to 7.6 MPa. For temperatures over the critical temperature of pure CO₂, the critical compositions and pressures of binary mixtures were approximated applying power laws with asymptotic behavior at critical point. The data were well correlated using the Peng-Robinson equation of state incorporating the generalized alpha function, with the Wong-Sandler mixing rules involving NRTL activity coefficient model. The experimental and correlated phase compositions were compared with Gibbs Ensemble Monte Carlo simulation data obtained at 293.15 K and 353.02 K. Though the molecular simulation predictions at low temperature (293.15 K) properly match experimental data, a slight shift appeared at high temperature (353.02 K), and the expected convergence of phase compositions near critical point was not fully observed.

Key words: Isothermal VLE data; R744; R-1234ze(E); Critical point; Modeling; Gibbs Ensemble Monte Carlo

NOMENCLATURE

a	Cohesive energy parameter ($\text{J m}^3 \text{mol}^{-2}$) or potential energy equation parameter (torsion)
ARD	Average relative deviation
b	Covolume parameter ($\text{m}^3 \text{mol}^{-1}$)
EoS	Equation of state
F	Objective function
g	Molar Gibbs energy (J.mol^{-1})
k_{ij}	Binary interaction parameter (BIP)
K	Potential energy parameter
N	Number of experimental data point
P	Pressure (MPa) / 1MPa = 10^6 Pa
PR	Peng-Robinson
q	Electrostatic charge
r	Bonding parameter
R	Gas constant ($\text{J mol}^{-1} \text{K}^{-1}$)
T	Temperature (K)
u	Uncertainty
v	Molar volume ($\text{m}^3 \text{mol}^{-1}$)
VLCC	vapor-liquid coexistence curve
x	Liquid mole fraction
y	Vapor mole fraction
Z	Compressibility factor
HFOs	Hydrofluoroolefins
GWP	Global warming potential

Greek letters

α	NRTL non randomness parameter
ω	Acentric factor
α	Relative volatility
σ	Standard deviation or Lennard-Jones distance at which the interaction potential is equal to zero
ε	Lennard-Jones energy parameter
θ	Bending angle
χ	Torsion (dihedral) angle

ρ	Molar density (mol m^{-3})
λ	Asymptotic law behavior parameter
μ	Asymptotic law behavior parameter
τ	NRTL parameter (J.mol^{-1})

Subscripts

c	Critical property
0	Reference state
cal	Calculated property
exp	Experimental property
i,j	Molecular species

Superscripts

V	Vapor phase
L	Liquid phase
E	Excess property

1. Introduction

In order to reduce greenhouse gas emissions and keep down the deterioration of the environmental situation, the refrigerant alternatives have become a hot topic in the refrigeration industry. The Montreal Protocol has decided to fully ban the use of chlorofluorocarbons (CFCs) with non-zero Ozone-Depleting Potential (ODP) and accelerate the phase-out of hydrochlorofluorocarbons (HCFCs) and hydrofluorocarbons (HFCs), which have zero ODP, but high Global Warming Potential (GWP). As a consequence, extensive researches have been performed to look for highly efficient alternative refrigerants with zero ODP and GWP lower than 150. Viable candidates for single-component are very limited [1]. The hydrofluoroolefins (HFOs), particularly R-1234yf (2,3,3,3-tetrafluoroprop-1-ene) and R-1234ze(E) (trans-1,3,3,3-tetrafluoroprop-1-ene), with zero ODP and low GWP are considered to be potential next-generation refrigerants [2] [3]. However, their mild flammability (ASHRAE classifies both R-1234yf and R-1234ze(E) in the A2L safety class [4]) blocks their practical applications. Carbon dioxide, a natural substance, presents several environmental and safety benefits such as zero ODP, low GWP, no toxicity and no flammability. These safety relevant characteristics were an essential reason for the initial widespread use and its renewed interest today, with subcritical

cascade plants and transcritical systems [5]. Despite its high volumetric cooling capacity, carbon dioxide shows defects in terms of thermodynamic properties, which can lead to a high system design complexity and low system coefficient of performance (COP). Also, actual refrigeration systems retrofit with pure carbon dioxide is unsuitable because of its relatively high discharge pressure. Consequently, the mixing of two refrigerants (CO₂ + HFO for instance) may give the opportunity to overcome the above concern.

Contrary to R-1234yf, R-1234ze(E) cannot be considered as a drop-in replacement of R-134a, due to lower volumetric cooling capacity [6], but instead should be considered when designing new equipment or adjusting existing one. However, the flammability characteristics of R-1234ze(E) (non-flammable below 30°C and zero burning velocity) are lower than other mildly flammable refrigerants like R-1234yf and R-32 [7], that makes R-1234ze(E) an interesting candidate for several medium-pressure and medium-temperature applications [8], and also as being a component of many refrigerant blends (R-450A, R-445A, and R-448A for instance). Therefore, the mixed refrigerant of CO₂+R-1234ze(E) has a good potential to be applied in refrigeration systems.

Indeed, the accurate knowledge of thermodynamic properties of a refrigerant is necessary to evaluate the performance of a refrigeration cycle, due to their direct relation to the energy balance equations [9]. Therefore, in order to help evaluating the relevance of this mixture for applications, the vapor liquid equilibrium properties of the binary mixture CO₂ + R-1234ze(E) should be experimentally investigated, as data concerning this mixture are very scarce.

Studies of phase behavior of binary systems involving CO₂, are the focus, such as CO₂ + R-32 [10] and CO₂ + R-152a [11], as well as the most promising mixtures currently composed of R-1234yf or R-1234ze(E) with either an HFC or a natural refrigerant [12] [13] [14] [15]. For the binary mixture CO₂ + R-1234yf, experimental data of vapor-liquid equilibrium and critical point have been studied by Juntarachat *et al.* [16].

To the knowledge of the authors, it exists only one paper concerning the experimental determination of thermodynamic properties concerning this binary system. Di Nicola *et al.* [15] have determined PVT_x properties using isochoric method. These data were not determined at equilibrium and consequently comparison with our new experimental data is very difficult. Moreover, these authors have done a data treatment of their using Carnahan and Starling [17] equation of state and compared prediction with data generated by molecular simulation by Raabe [18]. Barati-Harooni and Najafi-Marghmaleki [19] have also

used the data predicted by Raabe [18] to parametrize two equations of state: PC SAFT [20] and Peng Robinson EoS [21].

Besides the experimental investigation, molecular simulation methods have been used for several years to predict thermodynamic and transport properties of various pure compounds and mixtures. Vapor-Liquid Equilibrium (VLE) properties are preferentially studied using the Gibbs Ensemble Monte Carlo simulations (GEMC) [22], which allows direct computation of phase equilibrium by assigning each phase to its own simulation cell. The reliability of molecular simulation predictions depends mainly on the ability of the force field to reproduce different properties at different conditions. Since 2009, Raabe *et al.* [23] [24] [18] [6] have developed a transferable force field for different kinds of HFOs, and have shown its ability to reproduce VLE data for binary mixtures (with other HFOs, HFCs, or CO₂).

In this work, the phase behavior for the binary mixture CO₂ + R-1234ze(E) will be studied experimentally, and the experimental data will be fitted using a CTP in-house software (Thermopack) using Peng-Robinson equation of state [21] with generalized alpha function, Wong Sandler mixing rules [25] (to have a better representation of critical point) and NRTL activity coefficient model [26]. A comparison with Juntarachat *et al.* [16] critical data for binary system CO₂ + R-1234ze(E) will also be done. An attempt will be made to predict, via the GEMC molecular simulation technique, the coexistence curve experimental data at 293.15 K (at subcritical conditions, already studied by Raabe [18]) and at 353.02 K (at supercritical conditions for CO₂, and near-critical conditions for R-1234ze(E)) with the force field developed by Raabe *et al.* for R-1234ze(E) [24]), and the TraPPE force field [27] for CO₂. A comparison with experimental data indicates that the molecular models used for R-1234ze(E) and CO₂ in this work yield satisfactory VLE data.

2 Experimental principle

For the experiments in the present study, seven isothermal VLE measurements were considered: three below the critical temperature of CO₂ (283.32 K, 293.15 K and 298.15 K) and four above the critical temperature of CO₂ (308.13 K, 318.11 K, 333.01 K and 353.02 K). The measurements were performed using a static-analytic type apparatus with two electromagnetic capillary samplers Rapid On-Line Sampler-Injector (ROLSI®, patent FR 2.853.414) which offer precise micro-sampling of mixture

equilibrium phases and a gas chromatograph to analyze phase composition. For four temperatures above the critical temperature of pure CO₂, the critical phase behaviors of mixture were estimated at each temperature by using power laws with asymptotic behavior at critical point [28] [29] [30] [31] with the experimental data highly close to the critical point. VLE data were obtained using an equipment developed in CTP (Centre of Thermodynamics of Processes) research group. The experimental technique is based on static-analytic method [32].

2.1 Materials

CO₂ and R-1234ze(E) were respectively purchased from Air Liquide and Honeywell with a purity higher than 99.995 vol.% and 99.5 wt.% (Table 1). Except from degassing the sample before loading the products into the equilibrium cell, no further purification of the products was done.

Table 1: Chemical samples used for experimental work

Chemicals	CAS number	Supplier	Purity	Analysis method ^a
Carbon dioxide	124-38-9	Air Liquide	99.995 vol.%	GC
R-1234ze(E)	29118-24-9	Honeywell	99.5 wt.%	GC

^a GC: Gas Chromatography

Experimental vapor pressures of R-1234ze(E) were compared to ones calculated using REFPROP version 10.0 [33] to ensure the purity of the product (Table S1, provided in Supplementary Information). With a Mean Relative Deviation of the vapor pressure of 0.51%, the purity of the R-1234ze(E) has been verified.

2.2 Apparatus

An in-house developed apparatus based on a static-analytic method is used in this work to perform the VLE data measurement. The apparatus is the one already used by Madani *et al.* [34]. The equilibrium cell is comprised of a sapphire tube, which contains the mixture, sealed by two titanium flanges respectively at the top and bottom. Each flange is connected to a platinum resistance thermometer probe (Pt100, 100 Ω), and one outlet valve linked to a vacuum pump used for discharging, degassing and evacuation operations of the residual substance in the circuit. The top flange is joined in addition with two pressure transducers, two

inlet valves linked with two substance storage bottles, two electromagnetic capillary samplers ROLSI[®] set for withdrawing micro-samples of each phase without perturbing the thermodynamic equilibrium of the studied mixture and sending them to a gas chromatograph. The bottom flange holds besides a magnetic stirrer coupled with an electric motor, which accelerates the mass transfer between phases and reduces the time needed to achieve thermodynamic equilibrium. The equilibrium cell is immersed into a water thermoregulated liquid bath that provides and keeps the desired operating temperature within ± 0.01 K.

The pressure is measured by two pressure transducers (DRUCK, Model UNIK 500): one for low pressure (up to 5 MPa) and one for high pressure (up to 20 MPa). The pressure transducers were calibrated with respect to a pressure automated calibration equipment (PACE 5000, GE Sensing and Inspection Technologies). Pressure calibration uncertainties are estimated to be $U(P)=0.05$ kPa for the low-pressure transducer and $U(P)=0.06$ kPa for the high pressure transducer. The temperature is measured by two Pt100 platinum probes which are situated within each flange, i.e. the top and bottom flange. The temperature probes were calibrated against a standard probe (25 Ohms, TINSLEY, U.K.) which was certified by the ‘Laboratoire National d’Essai’ (Paris, France) based on the 1990 International Temperature Scale (ITS 90). The temperature difference between the top and the bottom of the cell is tested at the same time, and it should remain within the temperature uncertainties. Temperature calibration uncertainties are estimated to be $U(T)=0.01$ K and $U(T)=0.02$ K, respectively for bottom and upper probes, in the temperature scale 318.15 to 373.15 K.

Thermometers and pressure transducers are connected to an on-line data acquisition unit (HP34970A) which is linked to a computer.

The composition of each phase is analyzed by the Gas Chromatograph (Perichrom, PR 2100, France). The GC column is a 1% RT-1000 on Carbolblack B, 60/80 mesh supplied by Resteck, France. The Thermal Conductivity Detector (TCD) is used in this work. The calibration of TCD response was performed for each pure component using an automatic syringe (E-VOL[®]) which ensures a highly accurate injection volume. The vapor and liquid mole numbers calibration error is estimated to be $\pm 2.1\%$ for CO₂ and $\pm 2.0\%$ for R-1234ze(E). The uncertainties of mole fraction obtained from GC detector calibration are as shown in Eq. (1).

$$u_{cal}(x_1) = x_1 x_2 \sqrt{\left(\frac{u(n_1)}{n_1}\right)^2 + \left(\frac{u(n_2)}{n_2}\right)^2} \quad (1)$$

$$\text{with } x_1 = \frac{n_1}{n_1 + n_2}$$

where the subscript “cal” means “calibration”, n_1 is the mole number of compound 1, and n_2 the mole number of compound 2, and x_1 is liquid mole fraction of compound 1. In the case of vapor fractions, only the replacements of x_1 and x_2 by y_1 and y_2 are needed. The mole fraction uncertainties are less than $U(x, y) = 0.011$.

2.3 Experimental procedure

After connected all the components and checked the leak of whole system, the evacuation of the equilibrium cell and circuit was performed with a vacuum pump, which aimed at eliminating the inside residual air. The less volatile compound was at first loaded into the equilibrium cell at ambient temperature, that is R-1234ze(E) in this work. The equilibrium cell was then immersed in a thermostat liquid bath which provided the desired temperature. The desired temperature was assumed to be attained when the temperatures of the two Pt100 probes were unchanged and equivalent within the uncertainty for a while. The vapor pressure of R-1234ze(E) at desired temperature was recorded as first point of P - x - y diagram for binary system $\text{CO}_2 + \text{R-1234ze(E)}$. The second step was to inject the more volatile compound into the equilibrium cell, that is CO_2 , until the system pressure reaches the pressure desired and remains stable within the uncertainty for at least 10 min. The stirring is speeded up to reduce the thermodynamic equilibrium achieving time. Once the thermodynamic equilibrium was re-catched up, three purges of equilibrium content are made by the ROLSI[®] samplers. Then, samples from each phase are taken and sent to the GC for analysis. It should be noted that the frequency of sampling is decided during the GC conditions setting, and the opening time of sampler is needed to be defined for every analysis, to keep the sampler quantity within the range of detector calibration and capacity of analysis. The CO_2 is re-introduced, a new thermodynamic equilibrium at a higher pressure was obtained. The above steps repeated until the whole composition range was covered for a specific temperature.

For each equilibrium condition, two phase samples were both repeatedly withdrawn at least six times in order to examine the experiment reliability (standard deviation), which was determined by the statistical method recommended by NIST [35] as shown in Eq. (2).

$$\sigma(X) = \sqrt{\frac{1}{n(n-1)} \sum_1^n (X_i - \bar{X})^2} \quad (2)$$

where n is the number of measurements, X_i is the i th measurement of composition and \bar{X} is the arithmetic mean value of X . The temperature, pressure, calibrated composition averages were registered as the vapor-liquid-equilibrium values reported in this work.

Each isothermal P - x - y diagram is described by at least 7 points. For temperatures higher than the critical temperature of CO_2 , more measurements were conducted near the critical point of mixture, in order to study the near-critical phase behavior.

3. Simulation Method

3.1 Force fields

The structure of the compounds studied in this work, and the nomenclature used for the different atom types are shown in Figure 1. The R-1234ze(E) molecule was modelled using the force field for fluoropropenes, developed by Raabe [24] [18] [23] [6], which is fully flexible, with a Lennard-Jones (LJ) center and a partial electrostatic charge on each atom site. This model is developed to provide a good agreement with experimental data on the vapor-liquid coexistence curve (VLCC), vapor pressures, normal boiling point and critical properties for pure R-1234ze(E) [24] and was used to predict the VLE phase diagram of the binary mixture R-1234ze(E) + CO₂ [18]. For CO₂, we have employed the TraPPE model developed by Potoff and Siepmann [27], as done by Raabe [18] for the same binary mixture. In the TraPPE model, the calculation of intermolecular interaction is also based on LJ sites and fixed partial charges on the three atomic sites. Contrary to the fully flexible model for fluoropropenes, the TraPPE force field models CO₂ as a rigid molecule (C-O = 0.116 nm), with no intramolecular contribution to the potential energy. The numerical values of the intermolecular and intramolecular parameters for these potentials are given in Table S2 and Table S3 respectively, provided in Supplementary Information.

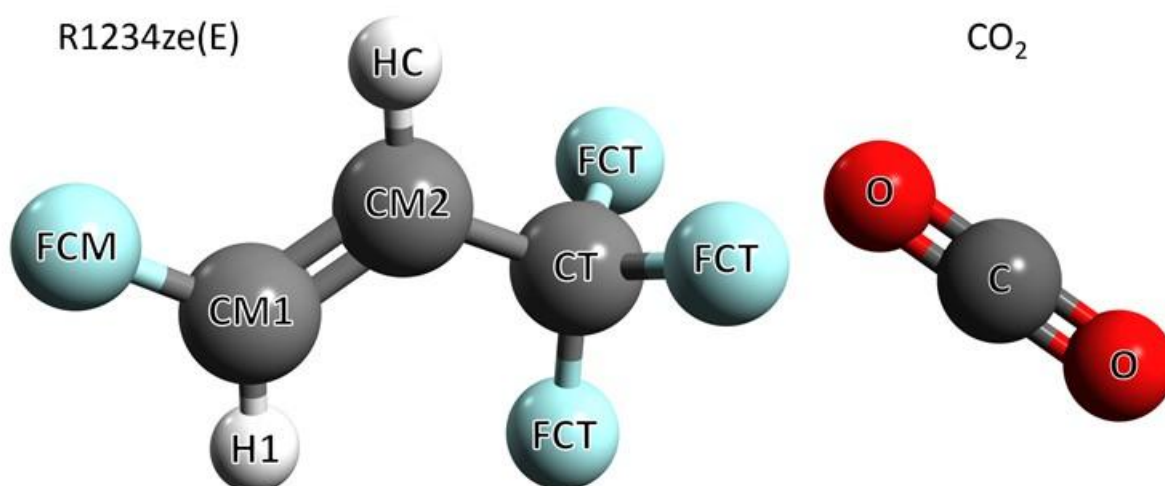


Figure 1: Structure of the compounds studied in this work: trans-1,3,3,3-tetrafluoro-1-propene (R-1234ze(E)) and carbon dioxide (CO₂), and nomenclature for the different atom types.

The potential energy is expressed by the following functional form (Eq. (3)).

$$\begin{aligned}
 U = & \\
 \sum_{\text{bonds}} \frac{K_r}{2} (r_{ij} - r_0)^2 & + \sum_{\text{angles}} \frac{K_\theta}{2} (\theta - \theta_0)^2 + \sum_{\text{dihedral}} \sum_0^8 a_n (\cos \chi)^n + \sum_i \sum_{j>i} \left\{ 4\varepsilon_{ij} \left[\left(\frac{\sigma_{ij}}{r_{ij}} \right)^{12} - \left(\frac{\sigma_{ij}}{r_{ij}} \right)^6 \right] + \frac{1}{4\pi\varepsilon_0} \frac{q_i q_j}{r_{ij}} \right\} \quad (3)
 \end{aligned}$$

Therein, the intramolecular potential energy is modelled by harmonic terms for bond stretching and angle bending, and an eighth-polynomial of the dihedral angle cosine. The torsion angle χ is null for a *trans* conformation. The non-bonded Lennard-Jones (LJ) and electrostatic interactions are considered between atoms separated by exactly three bonds, and are scaled by a factor of 1/2 and 1/1.2, whereas full LJ and electrostatic interactions are considered between atoms separated by more than three bonds. Dispersion-repulsion parameters between different atom types were obtained using the Lorentz-Berthelot combining rules (Eq. (4)).

$$\varepsilon_{ij} = \sqrt{\varepsilon_{ii}\varepsilon_{jj}}, \quad \sigma_{ij} = \frac{\sigma_{ii} + \sigma_{jj}}{2} \quad (4)$$

3.2 Algorithms

Isothermal VLE properties of the binary mixture CO₂ + R-1234ze(E) were calculated via Monte Carlo Gibbs ensemble [22] (GEMC) simulations in the isothermal-isobaric (NPT) ensemble using the in-house simulation code GIBBS, developed by IFPEN, CNRS and Université Paris-Sud [31]. Each phase is simulated within a box, or a cell, with periodic boundary conditions and minimum image convention, and molecules are transferred between the cells to equalize chemical potential. The cutoff radius for the LJ interactions was set to 1.2 nm, and standard long-range corrections were applied [36] [37]. The Ewald sum technique [38] [37] was employed to deal with electrostatic interactions with a cutoff radius set to 1.2 nm. CO₂ + R-1234ze(E) VLE data were calculated at 293.15 K and 353.02 K, to match thermodynamic conditions set for the experimental measurements presented in this paper. Nearly all the studied systems contained a total of 2000 molecules, except for the pressures close to the critical point, where the size of the

system was increased up to 4000 molecules. Configurational phase space was sampled at 293.15 K (respectively 353.02 K) by means of different Monte Carlo moves, with attempted probabilities of 12% for translations (resp. 20%), 6.5% for rotations (resp. 6.5%), 12% for bond stretching (resp. 20%), 12% for internal regrowths (resp. 20%), 12% for internal rotations (resp. 20%), 45% for molecule transfer between phases (resp. 13%), 0.5% for volume change (resp. 0.5%). The amplitudes of translation, rotation and volume changes are automatically adjusted during the simulation to achieve an acceptance ratio of 40%. Most of the simulations at 293.15 K were performed using 30 million Monte Carlo steps for the equilibration part and about 150 million Monte Carlo steps for the production part, where one Monte Carlo step corresponds to an attempted Monte Carlo move. At 353.02 K, the production part is about 30 to 80 million Monte Carlo steps.

4. Correlations

The critical temperatures (T_c), critical pressures (P_c) and acentric factors of each pure compound are taken from the REFPROP (Reference Fluid PROPERTIES) [33] computer database (version 10.0) and presented in Table 2.

Table 2: Critical parameters and acentric factors of CO₂ and R-1234ze(E) [33]

Compound	T_c (K)	P_c (MPa)	Acentric factor (ω)
CO ₂	304.13	7.377	0.224
R-1234ze(E)	382.51	3.635	0.313

As experimental data is acquired for $T < T_c(\text{CO}_2)$ and $T > T_c(\text{CO}_2)$, and as there is a well-known discontinuity of binary interaction parameters [39] [40], we have opted for an individual data processing for each temperature.

The Peng-Robinson Equation of State (PR EoS) (1978) [21] has been used to correlate the experimental data. This model was selected to represent experimental data, calculate the equilibrium properties at the critical point, and calculate the critical line to allow a comparison with the work of Juntaratchat et al. [16] on the critical line.

Statistical Associating Fluid Theory (SAFT) type models provide a good description of molecular interactions, but they were initially developed for long chain and for associating molecules. There may be

some dipole-dipole interaction with R-1234ze(E), but R-1234ze(E) and CO₂ are not associating molecules. It is right that the evolution of binary interaction parameters with temperature is better described by SAFT type models, but it is well known that SAFT type models are not good to calculate critical point [41]. It is still possible to correct the predicting capability of SAFT type models with crossover theory [42] [43]. Another possibility is to fit a parameter (exponent) of the Lennard-Jones intermolecular potential, as in SAFT Mie type models [44]. This correction adds two extra parameters and requires more data to fit them. As discussed by El Ahmar *et al.* [45], there is no improvement when compared to cubic EoS (and more parameters must be determined) for description of phase diagram. Thus, cubic EoS, such as PR EoS, are strongly preferred, if experimental data are available.

The Wong-Sandler (WS) mixing rules [25] were chosen (Eqs. (5) ~ (7)).

$$b = \frac{\sum_i \sum_j x_i x_j \left(b - \frac{a}{RT}\right)_{ij}}{1 - \left(\frac{\sum_i x_i \frac{a_i}{b_i}}{RT} + \frac{g^E(T, P = \infty, x_i)}{CRT}\right)} \quad (5)$$

$$b - \frac{a}{RT} = \sum_i \sum_j x_i x_j \left(b - \frac{a}{RT}\right)_{ij} \quad (6)$$

$$\left(b - \frac{a}{RT}\right)_{ij} = \frac{1}{2} \left[\left(b - \frac{a}{RT}\right)_i + \left(b - \frac{a}{RT}\right)_j \right] (1 - k_{ij}) \quad (7)$$

k_{ij} is a binary interaction parameter and $C = \ln(1/2)$. As shown by Coquelet *et al.* [46], the WS mixing rules yield good agreement with experimental phase compositions, even near the critical point.

The excess Gibbs energy is calculated using the NRTL [26] local composition model (Eq. (8)).

$$\frac{g^E(T, P, x_1)}{RT} = \sum_i x_i \sum_j \frac{x_j \exp\left(-\frac{\tau_{ji}}{RT}\right)}{\sum_k x_k \exp\left(-\frac{\tau_{ki}}{RT}\right)} \tau_{ji} \quad (8)$$

with $\tau_{ii} = 0$ and $\alpha_{ii} = 0$. α_{ji} , τ_{ji} ($\neq \tau_{ij}$) are adjustable parameters. It is recommended [26] to use $\alpha_{ji} = 0.3$ for systems like the one considered in the present paper. τ_{ji} is adjusted directly to VLE data through a modified Simplex algorithm [47] using the objective function given in Eq. (9). Calculations are based on a Flash TP-type algorithm.

$$F = \frac{100}{N} \left[\sum_1^N \left(\frac{x_{\text{exp}} - x_{\text{cal}}}{x_{\text{exp}}} \right)^2 + \sum_1^N \left(\frac{y_{\text{exp}} - y_{\text{cal}}}{y_{\text{exp}}} \right)^2 \right] \quad (9)$$

where N is the number of data points, x_{exp} and x_{cal} are respectively the measured and calculated liquid phase mole fractions, and y_{exp} and y_{cal} are respectively the measured and calculated vapor phase mole fractions. For temperatures higher than the critical temperature of CO_2 , the binary system conventionally has a critical point. Using the power laws with asymptotic behavior at critical point [29] [30] [31], at a given temperature, the mixture critical composition and pressures can be calculated (Eq. (10)) with the experimental data highly close to the critical point.

$$\begin{aligned}\frac{y+x}{2} - x_c &= \lambda_1(P_c - P) \\ y - x &= \lambda_2(P_c - P) + \mu(P_c - P)^\beta\end{aligned}\tag{10}$$

where x and y are molar fraction in the liquid and vapor phases when the system reaches the VLE at pressure P . $\beta = 0.325$ is a characteristic universal exponent (Sengers *et al.* [48]). λ_1 , λ_2 and μ are adjustable coefficients regressed from experimental VLE data near the critical point.

5. Results and discussion

5.1 Experimental data of Vapor-liquid equilibrium of the $\text{CO}_2 + \text{R-1234ze(E)}$ binary system

The experimental isothermal VLE data, measured at seven temperatures (283.31, 293.16, 298.18, 308.17, 318.85, 333.01 and 353.18 K) using the static-analytic type apparatus are reported in Table 3 and plotted in Figure 2. The adjusted parameters and the objective function values corresponding to our model are given in Table 4. Taking into account the evolution of the different Binary Interaction Parameters (BIP; τ_{12} , τ_{21} and k_{12}) with the temperature, we have also adjusted the BIP using data where temperature is higher than the critical temperature of CO_2 with no temperature dependency (see Table 4). The trends of these temperature-dependent binary parameters are plotted in Figures S1 to S3, provided in Supplementary

Information. Figure 3 presents the relative volatility (comparison between experimental and calculated values).

Table 3: Experimental isothermal VLE data for the CO₂ (1) + R-1234ze(E) (2) mixture system and their standard uncertainties $U(T) = 0.02$ K, $U(P) = 0.0006$ MPa, $U_{\max}(x, y) = 0.011$

$P_{\text{exp}}/\text{MPa}$	n	x_1	σ_{x_1}	n	$y_{1,\text{exp}}$	σ_{y_1}	$x_{1,\text{cal}}$	$y_{1,\text{cal}}$	Δx_1	Δy_1
<i>T: 283.32 K</i>										
0.3096		0.0000			0.0000					
1.0200	9	0.218	0.003	12	0.700	0.005	0.2266	0.7198	-0.0088	-0.0202
1.6960	11	0.411	0.002	9	0.8540	0.0008	0.4172	0.8513	-0.0059	0.0027
2.3860	12	0.588	0.004	11	0.9130	0.0008	0.5884	0.9119	-0.0009	0.0011
3.0680	12	0.746	0.001	11	0.9490	0.0005	0.7382	0.9480	0.0077	0.0011
3.7570	9	0.8764	0.0008	10	0.9725	0.0003	0.8727	0.9745	0.0037	-0.0020
<i>T: 293.15 K</i>										
0.4270		0.0000			0.0000					
0.8764	9	0.1204	0.0007	6	0.5159	0.0002	0.1205	0.5186	-0.0001	-0.0027
1.3700	8	0.2508	0.0002	11	0.7090	0.0003	0.2530	0.7047	-0.0022	0.0043
1.9200	8	0.3838	0.0006	8	0.8085	0.0002	0.3885	0.8035	-0.0047	0.0050
2.9890	6	0.6124	0.0008	8	0.8974	0.0001	0.6095	0.8971	0.0029	0.0003
3.9470	6	0.770	0.001	7	0.9422	0.0002	0.7704	0.9422	0.0000	0.0000
5.1080	8	0.9303	0.0008	8	0.9797	0.0002	0.9302	0.9806	0.0001	-0.0009
<i>T: 298.15 K</i>										
0.4983		0.0000			0.0000					
1.1710	6	0.1644	0.0006	7	0.5608	0.0002	0.1677	0.5826	-0.0033	-0.0218
1.5930	7	0.2719	0.0005	7	0.7074	0.0007	0.2679	0.7024	0.0040	0.0050
2.3840	6	0.4437	0.0004	6	0.8201	0.0001	0.4380	0.8171	0.0057	0.0030
3.1950	6	0.5882	0.0004	7	0.8794	0.0005	0.5881	0.8794	0.0001	0.0000
4.2030	7	0.7471	0.0004	8	0.9260	0.0002	0.7457	0.9273	0.0014	-0.0013
5.4320	6	0.8992	0.0006	7	0.9662	0.0007	0.9020	0.9684	-0.0028	-0.0022
<i>T: 308.13 K</i>										
0.6850		0.0000			0.0000					
1.4800	8	0.1677	0.0004	11	0.5329	0.0005	0.1675	0.5492	0.0002	-0.0163
2.3050	6	0.3319	0.0005	7	0.7240	0.0002	0.3242	0.7217	0.0077	0.0023
3.1010	9	0.4629	0.0006	6	0.8072	0.0002	0.4574	0.8047	0.0055	0.0025
4.0030	7	0.6044	0.0005	9	0.8656	0.0007	0.5901	0.8612	0.0143	0.0044
5.1600	8	0.7476	0.0004	7	0.9107	0.0004	0.7387	0.9080	0.0089	0.0027
5.6830	7	0.8049	0.0003	9	0.9264	0.0004	0.7993	0.9245	0.0056	0.0019
6.0440	6	0.8409	0.0004	6	0.9339	0.0001	0.8387	0.9350	0.0022	-0.0011
6.3520	7	0.8724	0.0004	7	0.9427	0.0003	0.8705	0.9436	0.0019	-0.0009
6.5070	9	0.8875	0.0005	6	0.9476	0.0005	0.8858	0.9478	0.0017	-0.0002
6.5970	6	0.8959	0.0002	6	0.9505	0.0006	0.8945	0.9503	0.0014	0.0002

6.7050	6	0.9049	0.0003	6	0.9531	0.0004	0.9047	0.9533	0.0002	-0.0002
6.9000	6	0.9220	0.0003	8	0.9587	0.0004	0.9225	0.9587	-0.0005	0.0000
7.0110	6	0.9321	0.0001	6	0.9625	0.0007	0.9322	0.9618	-0.0001	0.0007
7.1040	7	0.9396	0.0004	7	0.9644	0.0002	0.9401	0.9644	-0.0005	0.0000
7.2560	6	0.9515	0.0003	6	0.9681	0.0003	0.9525	0.9687	-0.0010	-0.0006
7.3680	6	0.9595	0.0001	4	0.9708	0.0002	0.9614	0.9718	-0.0019	-0.0010
7.4300	6	0.9641	0.0004	6	0.9719	0.0003	0.9663	0.9734	-0.0022	-0.0015
7.4620	7	0.9665	0.0002	7	0.9723	0.0002	0.9689	0.9742	-0.0024	-0.0018

T: 318.11 K

0.8730		0.0000			0.0000					
1.4780	6	0.1093	0.0002	5	0.3953	0.0002	0.1093	0.3953	0.0000	0.0000
1.9060	12	0.1846	0.0002	7	0.538	0.0008	0.1854	0.5312	-0.0008	0.0071
3.6370	5	0.4666	0.0002	6	0.7707	0.001	0.4543	0.7663	0.0123	0.0044
5.0220	6	0.6388	0.0002	7	0.8454	0.0001	0.6273	0.8427	0.0115	0.0027
6.0510	6	0.7432	0.0003	6	0.8798	0.0007	0.7382	0.8785	0.0050	0.0013
6.5050	7	0.7845	0.0005	7	0.8915	0.0002	0.7834	0.8910	0.0011	0.0005
6.8210	6	0.8172	0.0003	6	0.8994	0.0002	0.8137	0.8986	0.0035	0.0008
7.0220	6	0.8317	0.0003	6	0.9034	0.0001	0.8326	0.9030	-0.0009	0.0004
7.1040	7	0.8396	0.0001	6	0.9048	0.0001	0.8402	0.9047	-0.0006	0.0001
7.1990	6	0.8486	0.0002	6	0.9067	0.0002	0.8490	0.9065	-0.0004	0.0002
7.3060	6	0.8588	0.0005	6	0.9083	0.0002	0.8590	0.9084	-0.0002	-0.0001
7.4320	6	0.8703	0.0002	5	0.9091	0.0001	0.8709	0.9102	-0.0006	-0.0011
7.5620	6	0.8842	0.0001	7	0.9049	0.0003	0.8837	0.9113	0.0005	-0.0064
7.5950	6	0.8898	0.0004	6	0.9013	0.0005	0.8871	0.9114	0.0027	-0.0101

T: 333.01 K

1.2720		0.0000			0.0000					
1.9540	7	0.1034	0.0003	6	0.3243	0.0002	0.1058	0.3254	-0.0024	-0.0011
2.6980	7	0.2129	0.0002	7	0.5065	0.0003	0.2135	0.5031	-0.0006	0.0034
3.4780	6	0.3241	0.0006	7	0.6136	0.0001	0.3176	0.6108	0.0065	0.0028
4.4960	6	0.4531	0.0001	6	0.7026	0.0002	0.4412	0.6966	0.0119	0.0060
5.5620	6	0.5587	0.0003	6	0.7583	0.0004	0.5583	0.7524	0.0004	0.0059
6.3540	7	0.6367	0.0002	6	0.7822	0.0003	0.6394	0.7800	-0.0027	0.0022
6.6030	8	0.6646	0.0003	8	0.7893	0.0006	0.6644	0.7865	0.0002	0.0028
6.9880	7	0.7041	0.0003	7	0.7949	0.0004	0.7033	0.7940	0.0008	0.0009
7.0860	7	0.7121	0.0003	10	0.795	0.001	0.7135	0.7953	-0.0014	-0.0005
7.1830	6	0.7235	0.0003	6	0.7907	0.0008	0.7238	0.7962	-0.0003	-0.0055
7.2920	6	0.7334	0.0002	6	0.7879	0.0005	0.7358	0.7965	-0.0024	-0.0086
7.3530	8	0.7433	0.0002	7	0.7830	0.0004	0.7429	0.7963	0.0004	-0.0133

T: 353.02 K

2.0098		0.0000			0.0000					
2.5160	6	0.0629	0.0001	8	0.1636	0.0005	0.0631	0.1667	-0.0002	-0.0031
3.0560	6	0.1284	0.0001	6	0.2883	0.0008	0.1290	0.2893	-0.0006	-0.0010
3.5020	6	0.1795	0.0003	7	0.362	0.001	0.1820	0.3637	-0.0025	-0.0014
4.1440	6	0.2553	0.0002	8	0.4471	0.0009	0.2561	0.4431	-0.0008	0.0040

4.5380	6	0.3006	0.0002	7	0.4855	0.0007	0.3005	0.4803	0.0001	0.0052
5.0440	6	0.3591	0.0002	7	0.5243	0.0004	0.3567	0.5185	0.0024	0.0058
5.2650	5	0.3840	0.0002	7	0.5360	0.0006	0.3812	0.5322	0.0029	0.0038
5.4400	6	0.4045	0.0001	6	0.5462	0.0005	0.4006	0.5418	0.0040	0.0044
5.6220	6	0.4262	0.0002	7	0.5562	0.0004	0.4209	0.5507	0.0053	0.0056
5.8050	5	0.4480	0.0002	6	0.5634	0.0001	0.4416	0.5583	0.0064	0.0051
6.0140	6	0.4686	0.0002	6	0.5689	0.0002	0.4660	0.5653	0.0027	0.0036
6.1220	9	0.4781	0.0002	6	0.5683	0.0008	0.4790	0.5679	-0.0009	0.0004
6.2330	6	0.4900	0.0002	6	0.5656	0.0002	0.4931	0.5698	-0.0031	-0.0042
6.3450	7	0.5068	0.0002	7	0.5635	0.0002	0.5082	0.5704	-0.0014	-0.0069
6.3620	6	0.5070	0.0002	6	0.5617	0.0003	0.5107	0.5703	-0.0037	-0.0086

σ_{x_i} is the standard deviation (equation 2), n the number of samples

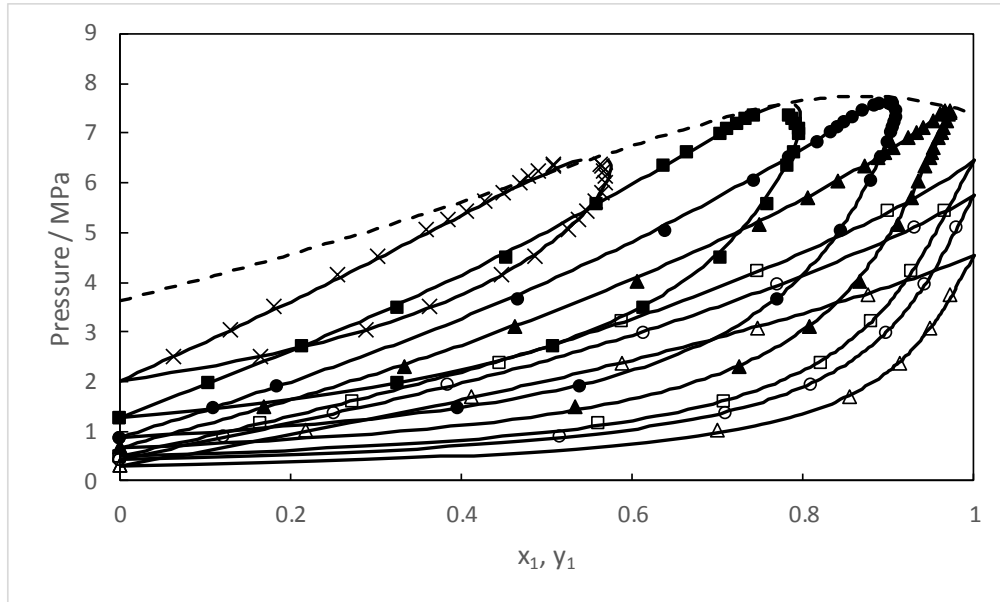


Figure 2: Pressure as a function of CO₂ mole fraction in the CO₂ (1) + R-1234ze(E) (2) mixture at different temperatures and critical line. Δ : 283.32 K, \circ : 293.15 K, \square : 298.15 K, \blacktriangle : 308.13 K, \bullet : 318.11 K, \blacksquare : 333.01 K, \times : 353.02 K. Solid lines: calculated with PR EoS, Wong-Sandler mixing rules and NRTL activity coefficient model with parameters from Table 4 (and corresponding parameters for $T > T_c(\text{CO}_2)$). Dashed line: calculated mixture critical line.

Table 4: Values of the binary interaction parameters and objective function at each temperature.

T/K	$\tau_{12}/\text{J}\cdot\text{mol}^{-1}$	$\tau_{21}/\text{J}\cdot\text{mol}^{-1}$	k_{12}	F
283.32	-8.264	287.3	0.2546	4.8
293.15	-2128	3492	0.2350	1.6
298.15	-1495	2321	0.2336	2.9
308.13	-2339	3568	0.2814	3.3
318.11	-2388	3667	0.2709	2.4

333.01	-441	693	0.2715	2.5
353.02	-36.71	511	0.2909	1.6
$T > T_c \text{ CO}_2$	-2137	3181	0.2757	3.1

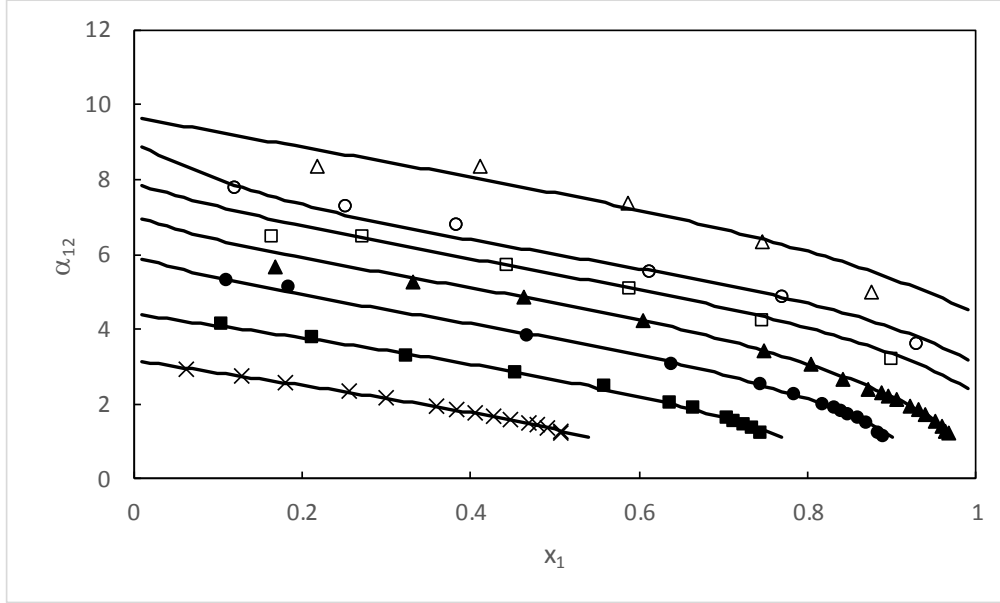


Figure 3: Relative volatility for the binary system the CO₂ (1) + R-1234ze(E) (2) mixture at different temperatures. Δ : 283.32 K, O: 293.15 K, \square : 298.15 K, \blacktriangle : 308.13 K, \bullet : 318.11 K, \blacksquare : 333.01 K, \times : 353.02 K. Solid lines: calculated with PR EoS, Wong-Sandler mixing rules and NRTL activity coefficient model with parameters from Table 4.

The BIP behavior differs in the subcritical and supercritical region relative to the critical temperature of pure CO₂. A discontinuity of BIP occurs at $T = T_c(\text{CO}_2)$. This phenomenon could be considered normal for all the binary systems [49].

Mean Absolute Deviation (MAD), Mean Relative Deviation (MRDU), and the BiasU, applied on pressures and vapor phase mole fractions, are defined by Eqs. (11), (12) and (13), respectively.

$$\text{MAD} = \frac{1}{N} \sum |U_{\text{cal}} - U_{\text{exp}}| \quad (11)$$

$$\text{MRDU} = \frac{100}{N} \sum \left| \frac{U_{\text{cal}} - U_{\text{exp}}}{U_{\text{exp}}} \right| \quad (12)$$

$$\text{BiasU} = \frac{100}{N} \sum \frac{U_{\text{exp}} - U_{\text{cal}}}{U_{\text{exp}}} \quad (13)$$

where N is the number of data points, and $U = x_1$ or y_1 . MRDU and BiasU indicators, which give information about the agreement between model and experimental results, are presented in Table 5.

Table 5: Mean Relative deviation MRDU and BiasU obtained in fitting experimental VLE data with PR EoS, Mathias-Copeman alpha function and WS mixing rules involving NRTL model.

T/K	BiasX %	MRDX %	BiasY %	MRDY %
283.32	-0.29	0.45	0.11	0.31
293.15	0.10	0.88	-0.53	0.89
298.15	0.10	0.88	-0.53	0.89
308.13	0.44	0.53	-0.12	0.31
318.11	0.38	0.48	0.04	0.32
333.01	0.11	0.71	-0.03	0.62
353.02	0.09	0.67	0.07	0.89
No temperature dependency ($T > T_c(\text{CO}_2)$)	-0.20	1.03	-0.11	0.55

Using our model, we have a good correlation of the experimental data. Moreover, by considering no temperature dependency of the BIP for $T > T_c(\text{CO}_2)$ we have a good representation of the experimental data. These parameters will be considered for the calculation of the critical line.

5.2 Predicted and experimental critical phase behavior data

The critical phase behavior data calculated by power laws with asymptotic behavior at critical point (Eq. (11)) are presented in Table 6 and plotted on Figures 4 and 5.

Table 6: Predictions using power laws with asymptotic behavior at critical point of critical compositions (x_c) and pressures (P_c) of the CO_2 (1) + R-1234ze(E) (2) binary system at four temperatures above the critical temperature of pure CO_2 .

T	P_c	x_c	λ_1	λ_2	μ
308.13	7.648	0.979	0.061	-0.051	-0.010
318.11	7.603	0.897	0.045	-0.047	0.054
331.01	7.399	0.765	0.032	-0.035	0.104
353.02	6.452	0.540	0.037	-0.052	0.110

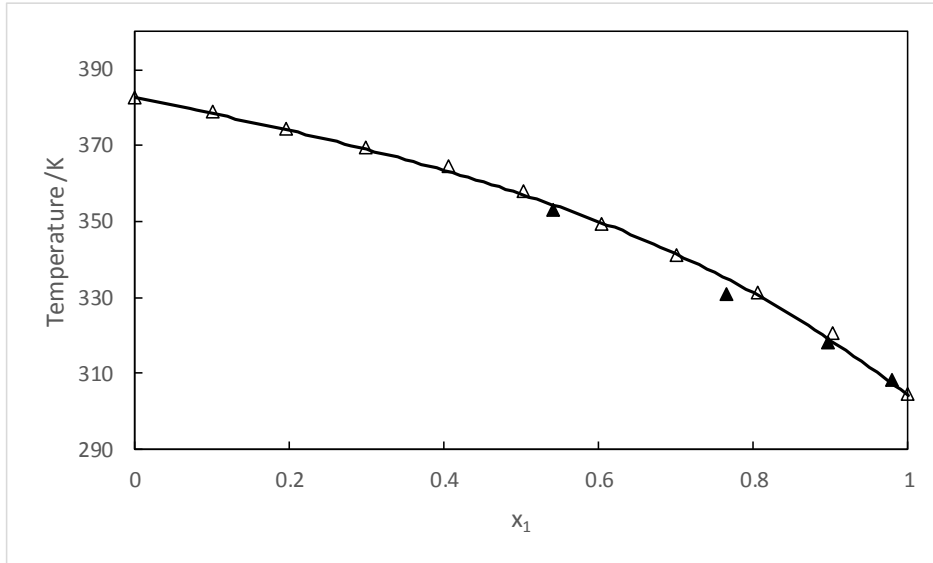


Figure 4: Critical temperature of the binary system CO₂ (1) + R-1234ze(E) (2). Solid line: calculated using our model. Δ : experimental data from Juntaratchat *et al.* [16], \blacktriangle : predicted using power laws with asymptotic behavior at critical point.

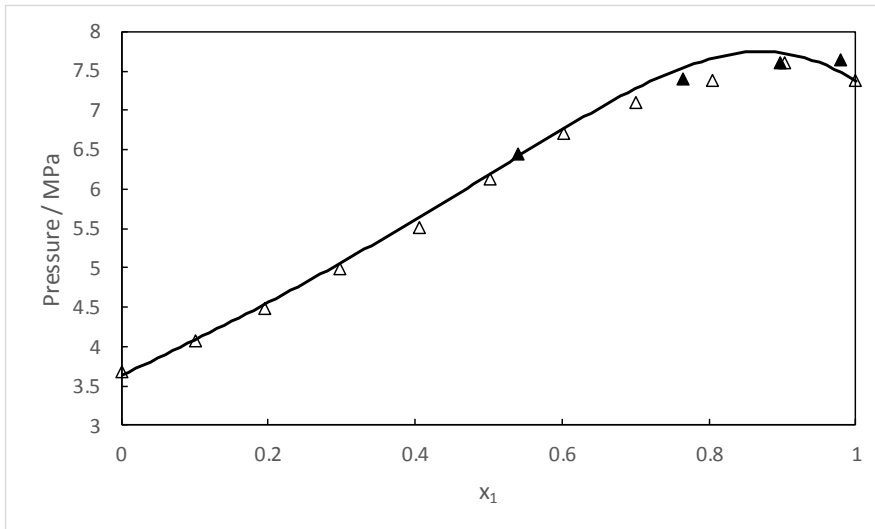


Figure 5: Critical pressure of the binary system CO₂ (1) + R-1234ze(E) (2). Solid line: calculated using our model. Δ : experimental data from Juntaratchat *et al.* [16], \blacktriangle : predicted using power laws with asymptotic behavior at critical point.

In Figures 4 and 5, the experimental data of the critical points for 11 compositions ($x(\text{CO}_2) = 0, 0.1002, 0.1946, 0.2977, 0.4053, 0.5016, 0.6033, 0.6997, 0.8057, 0.9024$ and 1) obtained by Juntaratchat *et al.* [16] through a synthetic-dynamic method and observation of critical opalescence are plotted for validating the prediction accuracy. A good agreement between the experimental and predicted data can be observed from

the Figures 4 and 5. The calculation of critical points was proposed by Heidemann and Khalil [50] in 1980 and Michelsen and Heidemann [51] in 1981. They have used Helmholtz energy as thermodynamic potential and considered that the critical point corresponds to the limit of stability. They developed an algorithm to calculate the critical point with a van der Waals type EoS, associated with the classical mixing rules. In 1998, Stockfleth and Dohrn [52] improved this method by generalizing the previous algorithm. We have chosen their algorithm to compute the critical line using our model. The binary parameters are thus obtained by fitting VLE data in the CO₂ supercritical domain (Table 4). Results are presented in Table 7 and plotted on Figures 4 and 5. Figure 2 presents the P - x - y phase diagram with all the isotherms and mixture critical line. The proposed model is in good agreement with experimental data and can predict the phase diagram of the system.

Table 7: Critical points calculated for the CO₂ (1) + R-1234ze(E) (2) system using our model.

x_{CO_2}	T/ K	P/MPa
0	382.5	3.64
0.1	378.4	4.08
0.2	373.9	4.56
0.3	369.0	5.07
0.4	363.5	5.61
0.5	357.2	6.18
0.6	350.0	6.75
0.7	341.4	7.27
0.8	331.1	7.65
0.9	318.8	7.73
1	304.1	7.38

5.3 GEMC simulations results on CO₂ + R-1234ze(E) binary system

The depiction of the GEMC simulation results VLE data for the CO₂+R-1234ze(E) binary system, plotted

in Figure 6 alongside corresponding experimental VLE data, attests the predictive ability of the force field models used in this work. The predicted phase compositions and phase densities for the CO₂ + R-1234ze(E) binary system at 293.15 and 353.02 K are reported in Table 8, as these properties can be obtained altogether from a GEMC simulation. The associated statistical uncertainties are calculated using a block-averaging method [36].

Table 8: GEMC simulation results for the Vapor Pressure P , Liquid-Phase Molar Fraction x , Gas-Phase Mole Fraction y , Saturated Liquid Density ρ^L and Saturated Vapor Density ρ^V of the VLE for the CO₂ (1) + R-1234ze(E) (2) mixture system^a

P /MPa	$u(P)$ /MPa	x_1	$u(x_1)$	y_1	$u(y_1)$	ρ^L /kg.m ⁻³	$u(\rho^L)$ /kg.m ⁻³	ρ^V /kg.m ⁻³	$u(\rho^V)$ /kg.m ⁻³
<i>T: 293.15 K</i>									
0.4405	0.0054	0		0		1197.0	3.3	22.88	0.31
0.87754	0.00078	0.1278	0.0016	0.5132	0.0043	1177.6	2.9	31.57	0.18
1.9219	0.0024	0.3850	0.0048	0.8054	0.0044	1115.6	4.9	53.60	0.48
3.9482	0.0061	0.7760	0.0032	0.9495	0.0013	963.9	4.5	105.14	0.72
5.648	0.059	1		1		796.8	6.6	169.9	3.8
<i>T: 353.02 K</i>									
2.176	0.054	0		0		935.8	6.4	125.4	4.2
2.483	0.031	0.04265	0.00067	0.1153	0.0047	920.9	3.9	133.5	6.1
3.302	0.092	0.1407	0.0012	0.3063	0.0091	898.7	9.3	167.0	8.4
4.466	0.100	0.2790	0.0038	0.476	0.011	835.7	3.8	205.2	9.2
5.623	0.080	0.38970	0.00096	0.551	0.010	794	10	281	19
6.130	0.022	0.4562	0.0028	0.6020	0.0068	710	12	275	13
6.377	0.018	0.4888	0.0051	0.6144	0.0067	660	13	290	18

^a $u(P)$, $u(x_1)$, $u(y_1)$, $u(\rho^L)$ and $u(\rho^V)$ are the statistical uncertainties for a 99% confidence interval (i.e. $k = 2.5$)

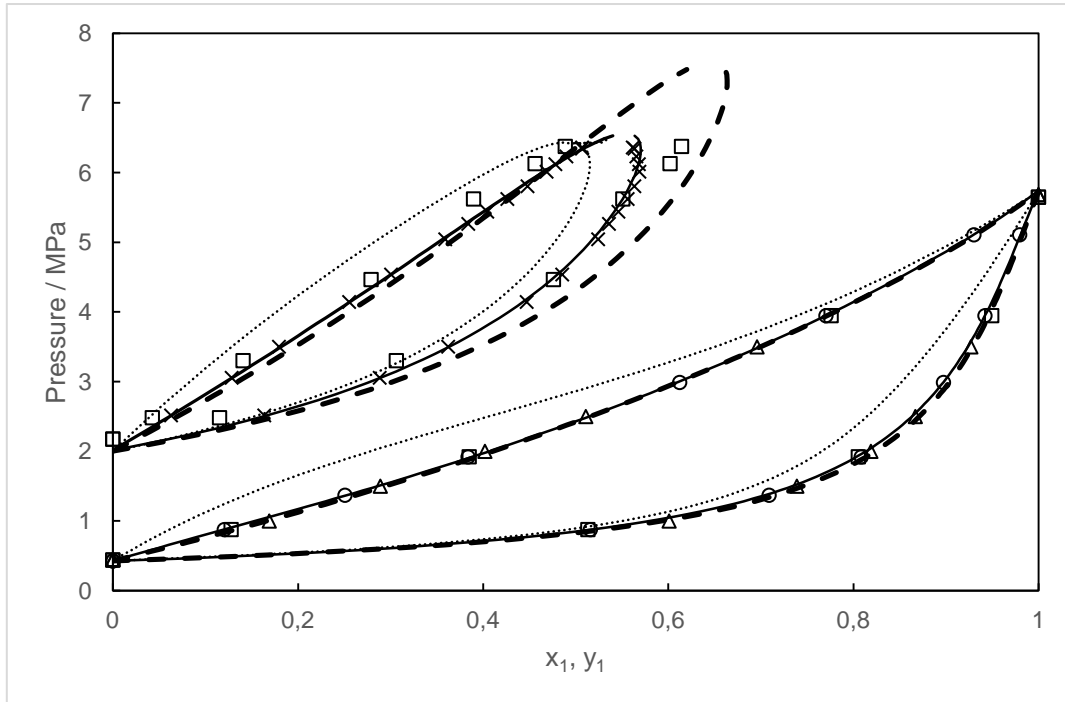


Figure 6: Pressure as a function of CO₂ mole fraction in the CO₂(1) + R-1234ze(E) (2) mixture at O: 293.15 K and ×: 353.02 K. □: GEMC simulations from this work. Δ: GEMC simulations from Raabe [18]. Solid lines: calculated with PR EoS, Wong-Sandler mixing rules and NRTL activity coefficient model with parameters from Table 4 (and corresponding parameters for $T > T_c(\text{CO}_2)$). Dotted line: calculated using REFPROP 9.0 [39]. Dashed line: calculated using REFPROP 10.0 [33].

At 293.15 K, MAD between GEMC simulation results and experimental data gives $\Delta P = 0.0014$ MPa, $\Delta x_1 = 0.0047$ and $\Delta y_1 = 0.0044$. This good agreement is consistent with Raabe studies on this system. At 353.02 K, whereas MAD between GEMC simulation results and experimental data gives $\Delta P = 0.072$ MPa, $\Delta x_1 = 0.026$ and $\Delta y_1 = 0.034$, the GEMC simulation vapor-liquid coexistence curves (VLCC) slightly overestimate experimental VLCC (setting aside the critical region). This may be related with the fact that the saturation pressure of pure R-1234ze(E) obtained by simulation, 2.176 ± 0.054 MPa, is higher than the experimental value, 2.0098 ± 0.0006 MPa.

Furthermore, while running simulations with twice the number of molecules, the critical region still shows convergence difficulties (inherent problem of the GEMC method discussed by Frenkel and Smit [37]), and molecular simulations fails to reproduce the dew point curve narrowing, occurring above 6 MPa in experimental data.

For the sake of comparison, Figure 6 also shows calculated VLCC from REFPROP version 9.0 and 10.0. For the mixture CO₂ + R-1234ze(E), for which no mixture data are available for binary pairs in REFPROP version 9.0 [53], an estimation scheme is used to approximate the interaction parameters. Such correlation

provides a qualitatively acceptable VLCC estimation, but misrepresents the bubble point curve for low CO₂ molar fraction, and the dew point curve for high CO₂ molar fraction, at 293.15 K. It also appears to be shifted from experimental VLCC (and breaking its shape near the critical point) at 353.02 K. With MAD of $\Delta x_1 = 0.071$ and $\Delta y_1 = 0.036$ at 293.15 K, and of $\Delta x_1 = 0.051$ and $\Delta y_1 = 0.037$ at 353.02 K, the calculated VLCC from REFPROP version 9.0 (with no fitted BIP) are less accurate than the GEMC simulation VLCC. In REFPROP version 10.0 [33], BIP have been fitted over Raabe's molecular simulation data [18] for the mixture CO₂ + R-1234ze(E), up to 310.92 K. Then, the correlation provides a perfectly fitting VLCC at 293.15 K, as Raabe provided data at this very temperature. On the other hand, at 353.02 K, it appears to have the dew point curve slightly shifted from experimental VLCC and to overestimate the critical point by 1 MPa. With MAD of $\Delta x_1 = 0.007$ and $\Delta y_1 = 0.008$ at 293.15 K, and of $\Delta x_1 = 0.008$ and $\Delta y_1 = 0.047$ at 353.02 K, the calculated VLCC from REFPROP version 10.0 (with fitted BIP) are more accurate than the REFPROP version 9.0 (with no fitted BIP) VLCC, but still falls short when extrapolated to higher temperature.

6. Conclusion

Isothermal (P - x - y) VLE data for CO₂ + R-1234ze(E) binary system were measured at seven temperatures ranging from 283.31 K to 353.16 K using a static-analytic method. The experimental data were given with the following uncertainties $U(T)=0.02$ K, $U(P)=0.0006$ MPa, and $U_{\max}(x,y)=0.011$ for molar composition fractions. Besides, the critical behaviour (P_c and x_c) were determined by power laws with asymptotic behavior at critical point and matched with experimental data in existing literature. Using the proposed model, it can be observed that the parameters τ_{12} , τ_{21} and k_{12} behave differently below and above the critical temperature of the lighter component (CO₂ in this work).

It is highly recommended to have parameters obtained on VLE data at temperatures above 304.13 K to calculate the critical locus line. The predicted critical locus line, obtained taking into account this remark,

is in very good agreement with the experimental (Juntarachat *et al.* [16]) and predicted (using power laws with asymptotic behaviour at critical point) data.

VLE data were also calculated from GEMC molecular simulations, performed at 293.15 and 353.02 K. The simulation studies were based on Raabe force field for R-1234ze(E) [24] and the TraPPE [27] force field for CO₂. Since no adjusted interaction parameter was used between unlike atom types, all GEMC simulation results for the mixtures were purely predictive. Comparison with experimental data indicates that the molecular models used for R-1234ze(E) and CO₂ yield reliable VLE predictions at low temperature. At 353.02 K, as CO₂ is supercritical, and R-1234ze(E) is close to its critical temperature, the critical region remains hard to properly predict with molecular simulations. The research results in the present study show that molecular simulation can be greatly helpful in the working fluid design.

7. Acknowledgement

MINES ParisTech and Shanghai Jiao Tong University (SPEIT) are acknowledged for funding S. Wang's internship.

8. Supplementary Information

Supplementary information related to this article can be found at:

<https://doi.org/10.1016/j.ijrefrig.2018.10.032>

9. REFERENCES

- [1] M. O. McLinden, J. S. Brown, R. Brignoli, A. F. Kazakov and P. A. Domanski, "Limited options for low-global-warming-potential refrigerants," *Nature Communications*, vol. 8, p. 14476, 2017.
- [2] M. Javadi, R. Sondergaard, O. Nielsen, M. Hurley and T. Wallington, "Atmospheric chemistry of trans-CF₃CH=CHF: products and mechanisms of hydroxyl radical and chlorine atom initiated oxidation," *Atmospheric Chemistry and Physics*, vol. 8, no. 12, pp. 3141-3147, 2008.
- [3] O. J. Nielsen, M. S. Javadi, M. S. Andersen, M. Hurley, T. J. Wallington and R. Singh, "Atmospheric

- chemistry of CF₃CFCH₂: Kinetics and mechanisms of gas-phase reactions with Cl atoms, OH radicals, and O₃," *Chemical Physics Letters*, pp. 18-22, 2007.
- [4] American Society of Heating, Refrigerating and Air-Conditioning Engineers, *ASHRAE Standard : Standards for Natural and Mechanical Ventilation*, New York : The Society: Print, 1973.
- [5] Bitzer, 12 October 2016. [Online]. Available: https://www.bitzer.de/shared_media/documentation/a-501-19.pdf. [Accessed 1 August 2018].
- [6] G. Raabe, "Molecular simulation studies in hydrofluoroolefine (HFO) working fluids and their blends," *Science and Technology for the Built Environment*, vol. 22, no. 8, pp. 1077-1089, 2016.
- [7] A. Mota-Babiloni, J. Navarro-Esbrì, F. Molès, À. Cervera, Barragàn, B. Peris and G. Verdù, "A review of refrigerant R1234ze (E) recent investigations," *Applied Thermal Engineering*, vol. 95, pp. 221-222, 2016.
- [8] P. Gullo and G. Cortella, "Theoretical evaluation of supermarket refrigeration systems using R1234ze(E) as an alternative to high-global warming potential refrigerants," *Science and Technology for the Built Environment*, vol. 22, no. 8, pp. 1145-1155, 2016.
- [9] C. Coquelet and D. Richon, "Experimental determination of phase diagram and modeling: Application to refrigerant mixtures," *International journal of refrigeration*, vol. 32, no. 7, pp. 1604-1614, 2009.
- [10] F. Rivollet, A. Chapoy, C. Coquelet and D. Richon, "Vapor-liquid equilibrium data for the carbon dioxide (CO₂)+ difluoromethane (R32) system at temperatures from 283.12 to 343.25 K and pressures up to 7.46 MPa," *Fluid phase equilibria*, vol. 218, no. 1, pp. 95-101, 2004.
- [11] H. Madani, A. Valtz, C. Coquelet, A. H. Meniai and D. Richon, "Vapor-liquid equilibrium data for the (hexafluoroethane+ 1, 1, 1, 2-tetrafluoroethane) system at temperatures from 263 to 353K and pressures up to 4.16 MPa," *Fluid Phase Equilibria*, vol. 268, no. 1, pp. 68-73, 2008.
- [12] T. Kamiaka, C. Dang and E. Hihara, "Vapor-liquid equilibrium measurements for binary mixtures of R1234yf with R32, R125, and R134a," *International Journal of Refrigeration*, vol. 36, no. 3, pp. 965-971, 2013.
- [13] P. Hu, L.-X. Chen and Z.-S. Chen, "Vapor-liquid equilibria for the 1, 1, 1, 2-tetrafluoroethane (HFC-134a)+ 1, 1, 1, 2, 3, 3, 3-heptafluoropropane (HFC-227ea) and 1, 1, 1-trifluoroethane (HFC-143a)+ 2, 3, 3, 3-tetrafluoroprop-1-ene (HFO-1234yf) systems," *Fluid Phase Equilibria*, vol. 360, pp. 293-297, 2013.
- [14] G. Di Nicola, C. Di Nicola, A. Arteconi and R. Stryjek, "PVTx measurements of the carbon dioxide+ 2, 3, 3, 3-Tetrafluoroprop-1-ene binary system," *Journal of Chemical & Engineering Data*, vol. 57, no. 2, pp. 450-455, 2012.
- [15] G. Di Nicola, G. Passerini, F. Polonara and R. Stryjek, "PVTx measurements of the carbon dioxide+trans-1, 3, 3, 3-tetrafluoroprop-1-ene binary system," *Fluid Phase Equilibria*, vol. 360, pp. 124-128, 2013.
- [16] N. Juntarachat, A. Valtz, C. Coquelet, R. Privat and J.-N. Jaubert, "Experimental measurements and correlation of vaporeliquid equilibrium and critical data for the CO₂ + R1234yf and CO₂ + R1234ze (E) binary mixtures," *International Journal of Refrigeration*, vol. 47, no. 141, p. e152, 2014.
- [17] R. De Santis, F. Gironi and L. Marrelli, "Vapor-liquid equilibrium from a hard-sphere equation of state," *Industrial & Engineering Chemistry Fundamentals*, vol. 15, no. 3, pp. 183-189, 1976.
- [18] G. Raabe, "Molecular simulation studies on the vapor-liquid phase equilibria of binary mixtures of

- R-1234yf and R-1234ze (E) with R-32 and CO₂," *Journal of Chemical & Engineering Data*, vol. 58, no. 6, pp. 1867-1873, 2013.
- [19] A. Barati-Harooni and A. Najafi-Marghmaleki, "Prediction of vapor-liquid equilibrium for binary mixtures containing R1234yf or R1234ze (E)," *International Journal of Refrigeration*, vol. 88, pp. 239-247, 2018.
- [20] J. Gross and G. Sadowski, "Perturbed-chain SAFT: An equation of state based on a perturbation theory for chain molecules," *Industrial & engineering chemistry research*, vol. 40, no. 4, pp. 1244-1260, 2001.
- [21] D.-Y. Peng and D. B. Robinson, "A new two-constant equation of state," *Industrial & Engineering Chemistry Fundamentals*, vol. 15, no. 1, pp. 59-64, 1976.
- [22] A. Z. Panagiotopoulos, "Direct determination of phase coexistence properties of fluids by Monte Carlo simulation in a new ensemble," *Molecular Physics*, vol. 61, no. 4, pp. 813-826, 1987.
- [23] G. Raabe and E. J. Maginn, "Molecular Modeling of the Vapor- Liquid Equilibrium Properties of the Alternative Refrigerant 2, 3, 3, 3-Tetrafluoro-1-propene (HFO-1234yf)," *The Journal of Physical Chemistry Letters*, vol. 1, no. 1, pp. 93-96, 2009.
- [24] G. Raabe, "Molecular modeling of fluoropropene refrigerants," *The Journal of Physical Chemistry B*, vol. 116, no. 19, pp. 5744-5751, 2012.
- [25] D. S. H. Wong and S. I. Sandler, "A theoretically correct mixing rule for cubic equations of state," *AIChE Journal*, vol. 38, no. 5, pp. 671-680, 1992.
- [26] H. Renon and J. M. Prausnitz, "Local compositions in thermodynamic excess functions for liquid mixtures," *AIChE journal*, vol. 14, no. 1, pp. 135-144, 1968.
- [27] J. J. Potoff and J. I. Siepmann, "Vapor-liquid equilibria of mixtures containing alkanes, carbon dioxide, and nitrogen," *AIChE journal*, vol. 47, no. 7, pp. 1676-1682, 2001.
- [28] I. L. Spain and J. Paauwe, *High Pressure Technology*, vol. 2, CRC Press, 1977.
- [29] J. Rainwater and F. Williamson, "Vapor-liquid equilibrium of near-critical binary alkane mixtures," *International Journal of Thermophysics*, vol. 7, no. 1, pp. 65-74, 1986.
- [30] M. R. Moldover and J. C. Rainwater, "Interfacial tension and vapor-liquid equilibria in the critical region of mixtures," *The Journal of chemical physics*, vol. 88, no. 12, pp. 7772-7780, 1988.
- [31] P. Ungerer, B. Tavitian and A. Boutin, *Applications of molecular simulation in the oil and gas industry: Monte Carlo methods*, Editions Technip, 2005.
- [32] R. Dohrn and G. Brunner, "High-pressure fluid-phase equilibria: experimental methods and systems investigated (1988-1993)," *Fluid Phase Equilibria*, vol. 106, no. 1-2, pp. 213-282, 1995.
- [33] E. W. Lemmon, I. Bell, M. L. Huber and M. O. McLinden, *NIST Standard Reference Database 23: Reference Fluid Thermodynamic and Transport Properties-REFPROP, Version 10.0*, National Institute of Standards and Technology, 2018.
- [34] H. Madani, A. Valtz, F. Zhang, J. El Abbadi, C. Houriez, P. Paricaud and C. Coquelet, "Isothermal vapor-liquid equilibrium data for the trifluoromethane (R23)+ 2, 3, 3, 3-tetrafluoroprop-1-ene (R1234yf) system at temperatures from 254 to 348 K," *Fluid Phase Equilibria*, vol. 415, pp. 158-165, 2016.
- [35] B. N. Taylor and C. E. Kuyatt, *Guidelines for evaluating and expressing the uncertainty of NIST measurement results*, Citeseer, 1994.

- [36] M. Allen and D. Tildesley, *Molecular Simulation of Liquids*, Clarendon, Oxford, 1987.
- [37] B. Smit and D. Frenkel, *Understanding molecular simulation: from algorithms to applications*, New York: Academic Press, 1996.
- [38] P. P. Ewald, "The calculation of optical and electrostatic grid potential," *Ann. Phys*, vol. 64, no. 3, pp. 253-287, 1921.
- [39] A. Valtz, C. Coquelet, A. Baba-Ahmed and D. Richon, "Vapor-liquid equilibrium data for the propane+ 1, 1, 1, 2, 3, 3, 3-heptafluoropropane (R227ea) system at temperatures from 293.16 to 353.18 K and pressures up to 3.4 MPa," *Fluid phase equilibria*, vol. 202, no. 1, pp. 29-47, 2002.
- [40] F. Rivollet, A. Chapoy, C. Coquelet and D. Richon, "Vapor-liquid equilibrium data for the carbon dioxide (CO₂)+ difluoromethane (R32) system at temperatures from 283.12 to 343.25 K and pressures up to 7.46 MPa," *Fluid Phase Equilibria*, vol. 218, no. 1, pp. 95-101, 2004.
- [41] W. A. Fouad and L. F. Vega, "Next generation of low global warming potential refrigerants: Thermodynamic properties molecular modeling," *AIChE Journal*, vol. 64, no. 1, pp. 250-262, 2018.
- [42] J. Janeček, P. Paricaud, M. Dicko and C. Coquelet, "A generalized Kiselev crossover approach applied to Soave-Redlich-Kwong equation of state," *Fluid Phase Equilibria*, vol. 401, pp. 16-26, 2015.
- [43] M. Dicko and C. Coquelet, "Application of a new crossover treatment to a generalized cubic equation of state," *Fluid Phase Equilibria*, vol. 302, no. 1-2, pp. 241-248, 2011.
- [44] S. Dufal, V. Papaioannou, M. Sadeqzadeh, T. Pogiatis, A. Chremos, C. S. Adjiman, G. Jackson and A. Galindo, "Prediction of thermodynamic properties and phase behavior of fluids and mixtures with the SAFT- γ Mie group-contribution equation of state," *Journal of Chemical & Engineering Data*, vol. 59, no. 10, pp. 3272-3288, 2014.
- [45] E. El Ahmar, A. Valtz, P. Paricaud, C. Coquelet, L. Abbas and W. Rached, "Vapour-liquid equilibrium of binary systems containing pentafluorochemicals from 363 to 413 K: Measurement and modelling with Peng-Robinson and three SAFT-like equations of states," *International Journal of Refrigeration*, vol. 35, no. 8, pp. 2297-2310, 2012.
- [46] C. Coquelet, A. Chareton, A. Valtz, A. Baba-Ahmed and D. Richon, "Vapor-Liquid Equilibrium Data for the Azeotropic Difluoromethane+ Propane System at Temperatures from 294.83 to 343.26 K and Pressures up to 5.4 MPa," *Journal of Chemical & Engineering Data*, vol. 2, no. 48, pp. 317-323, 2003.
- [47] E. Åberg and A. Gustavsson, "Design and evaluation of modified simplex methods," *Analytica chimica acta*, vol. 144, pp. 39-53, 1982.
- [48] J. V. Sengers, R. Kayser, C. Peters and H. White, *Equations of state for fluids and fluid mixtures*, vol. 5, Elsevier, 2000.
- [49] A. Valtz, C. Coquelet, A. Baba-Ahmed and D. Richon, "Vapor-liquid equilibrium data for the CO₂+ 1, 1, 1, 2, 3, 3, 3-heptafluoropropane (R227ea) system at temperatures from 276.01 to 367.30 K and pressures up to 7.4 MPa," *Fluid phase equilibria*, vol. 207, no. 1-2, pp. 53-67, 2003.
- [50] R. A. Heidemann and A. M. Khalil, "The calculation of critical points," *AIChE journal*, vol. 26, no. 5, pp. 769-779, 1980.
- [51] M. L. Michelsen and R. A. Heidemann, "Calculation of critical points from cubic two-constant equations of state," *AIChE journal*, vol. 27, no. 3, pp. 521-523, 1981.
- [52] R. Stockfleth and R. Dohrn, "An algorithm for calculating critical points in multicomponent mixtures which can easily be implemented in existing programs to calculate phase equilibria," *Fluid phase*

equilibria, vol. 145, no. 1, pp. 43-52, 1998.

[53] E. W. Lemmon, M. L. Huber and M. O. McLinden, *NIST Standard Reference Database 23: Reference Fluid Thermodynamic and Transport Properties-REFPROP, Version 9.0, National Institute of Standards and Technology*, 2013.

List of Tables

Table 1: Chemical samples used for experimental work

Table 2: Critical parameters and acentric factors of CO₂ and R-1234ze(E) [33].

Table 3: Experimental isothermal VLE data for the CO₂ (1) + R-1234ze(E) (2) mixture system and their standard uncertainties $U(T) = 0.02$ K, $U(P) = 0.0006$ MPa, $U_{\max}(x, y) = 0.011$

Table 4: Values of the binary interaction parameters and objective function at each temperature.

Table 5: Mean Relative deviation MRDU and BiasU obtained in fitting experimental VLE data with PR EoS, Mathias-Copeman alpha function and WS mixing rules involving NRTL model.

Table 6: Predictions using power laws with asymptotic behavior at critical point of critical compositions (x_{c1}) and pressures (P_c) of the CO₂ (1) + R-1234ze(E) (2) binary system at four temperatures above the critical temperature of pure CO₂.

Table 7: Critical points calculated for the CO₂ (1) + R-1234ze(E) (2) system using our model.

Table 8: GEMC simulation results for the Vapor Pressure P , Liquid-Phase Molar Fraction x , Gas-Phase Mole Fraction y , Saturated Liquid Density ρ^L and Saturated Vapor Density ρ^V of the VLE for the CO₂ (1) + R-1234ze(E) (2) mixture system^a

List of Figures

Figure 1: Structure of the compounds studied in this work: trans-1,3,3,3-tetrafluoro-1-propene (R-1234ze(E)) and carbon dioxide (CO₂), and nomenclature for the different atom types.

Figure 2: Pressure as a function of CO₂ mole fraction in the CO₂ (1) – R-1234ze(E) (2) mixture at different temperatures and critical line. Δ : 283.32 K, O: 293.15 K, \square : 298.15 K, \blacktriangle : 308.13 K, \bullet : 318.11 K, \blacksquare : 333.01 K, \times : 353.02 K. Solid lines: calculated with PR EoS, Wong-Sandler mixing rules and NRTL activity coefficient model with parameters from Table 4 (and corresponding parameters for $T > T_c(\text{CO}_2)$). Dashed line: calculated mixture critical line.

Figure 3: Relative volatility for the binary system the CO₂ (1) + R-1234ze(E) (2) mixture at different temperatures. Δ : 283.32 K, O: 293.15 K, \square : 298.15 K, \blacktriangle : 308.13 K, \bullet : 318.11 K, \blacksquare : 333.01 K, \times : 353.02 K. Solid lines: calculated with PR EoS, Wong-Sandler mixing rules and NRTL activity coefficient model with parameters from Table 4.

Figure 4: Critical temperature of the binary system CO₂ (1) + R-1234ze(E) (2). Solid line: calculated using our model. Δ : experimental data from Juntarachat *et al.* [16], \blacktriangle : predicted using power laws with asymptotic behavior at critical point.

Figure 5: Critical pressure of the binary system CO₂ (1) + R-1234ze(E) (2). Solid line: calculated using our model. Δ : experimental data from Juntarachat *et al.* [16], \blacktriangle : predicted using power laws with asymptotic behavior at critical point.

Figure 6: Pressure as a function of CO₂ mole fraction in the CO₂ (1) + R-1234ze(E) (2) mixture at O:

293.15 K and \times : 353.02 K. \square : GEMC simulations from this work. Δ : GEMC simulations from Raabe [18]. Solid lines: calculated with PR EoS, Wong-Sandler mixing rules and NRTL activity coefficient model with parameters from Table 4 (and corresponding parameters for $T > T_c(\text{CO}_2)$). Dotted line: calculated using REFPROP 9.0 [53]. Dashed line : calculated using REFPROP 10.0 [33].

Vapor-liquid equilibrium and molecular simulation data for carbon dioxide (CO₂) + trans-1,3,3,3-tetrafluoroprop-1-ene (R-1234ze(E)) mixture at temperatures from 283.32 to 353.02 K and pressures up to 7.6 MPa

Siyi Wang^{1,2}, Rémi Fauve², Christophe Coquelet^{2*}, Alain Valtz², Céline Houriez², Pierre-Arnaud Artola^{3a},
Elise El Ahmar², Bernard Rousseau^{3b} and Haitao Hu¹

1 Institute of Refrigeration and Cryogenics, Shanghai Jiao Tong Univ, 800 Dongchuan Rd, 200240
Shanghai, China

2 Mines ParisTech, PSL Research University, CTP – Centre of Thermodynamics of Processes 35, rue Saint
Honoré 77305 Fontainebleau Cedex France

3a : Laboratoire de Chimie Physique, Université Paris-Sud bâtiment 349, 310 Rue Michel Magat, 91405
Orsay, France

3b : Laboratoire de Chimie Physique, Université Paris-Sud bâtiment 349, UMR 8000 CNRS, 310 Rue
Michel Magat, 91405 Orsay, France

* : Corresponding author : christophe.coquelet@mines-paristech.fr (tel :+33164694962 Fax :+33164694968).

SUPPLEMENTARY INFORMATION

The material presented here is relevant to the conclusion of the paper but is not included in the printed
version for reason of space.

List of Tables

Table S1: Vapor pressures of R-1234ze(E)

Table S2: Intermolecular parameters [1] [2]

Table S3: Intramolecular parameters for R-1234ze(E) [2]

List of Figures

Figure S1: τ_{12} binary parameter as a function of temperature. Vertical dashed: CO₂ critical temperature.
Horizontal dashed line: parameter value obtained after considering all the data for $T > T_c(\text{CO}_2)$.

Figure S2: τ_{21} binary parameter as a function of temperature. Vertical dashed line: CO₂ critical temperature.
Horizontal dashed line: parameter value obtained after considering all the data for $T > T_c(\text{CO}_2)$.

Figure S3: k_{12} binary parameter as a function of temperature. Vertical dashed line: CO₂ critical temperature.
Horizontal dashed line: parameter value obtained after considering all the data for $T > T_c(\text{CO}_2)$.

Table S1: Vapor pressures of R-1234ze(E)

T (K)	P_{sat} (MPa)		MRD P_{sat} %
	Experiment	REFPROP [3]	
283.32	0.3096	0.3101	0.17
293.15	0.4270	0.4273	0.08
298.15	0.4983	0.4985	0.04
308.13	0.6850	0.6670	2.62
318.11	0.8730	0.8752	0.25
333.01	1.2720	1.2723	0.02
353.02	2.0098	2.0021	0.38

Table S2: Intermolecular parameters (converted values from TraPPE [1] and Raabe's force field [2])

Atom type	Lennard-Jones		Electrostatic charge
	σ [Å]	ϵ [kJ.mol ⁻¹]	q [e]
CO ₂			
C	2.80	0.22449074	0.70
O	3.05	0.65684329	-0.35
R-1234ze(E)			
CM1	3.40	0.41000	0.25325
CM2	3.40	0.41000	-0.48504
CT	3.40	0.31091	0.77614
FCM	2.90	0.23617	-0.19161
FCT	2.94	0.23617	-0.24329
HC	2.65	0.06570	0.24464
H1	2.47	0.06570	0.13249

Table S3: Intramolecular parameters for R-1234ze(E) (converted values from Raabe's force field [2])

Bonding parameters	r_0 [Å]	K_r [kJ.mol ⁻¹ .Å ⁻²]		
CM1-CM2	1.331	5663.38		
CM1-FCM	1.330	3729.46		
CM1-H1	1.086	3254.14		
CM2-HC	1.086	3254.14		
CM2-CT	1.511	2657.68		
CT-FCT	1.353	3089.22		
Bending parameters	θ_0 [rad]	K_θ [kJ.mol ⁻¹ .rad ⁻²]		
H1-CM1-CM2	2.104867078	304.18		
HC-CM2-CM1	2.104867078	304.18		
HC-CM2-CT	2.008873969	270.54		
H1-CM1-FCM	1.984439460	428.72		
CM2-CM1-FCM	2.139773663	422.76		
CM1-CM2-CT	2.165953602	419.40		
CM2-CT-FCT	1.942551457	626.34		
FCT-CT-FCT	1.876228946	735.22		
Torsion parameters ^a	a_0 [kJ.mol ⁻¹]	a_1 [kJ.mol ⁻¹]	a_2 [kJ.mol ⁻¹]	a_3 [kJ.mol ⁻¹]
H1-CM1-CM2-HC	27.8400	-27.8400	0.0000	0.0000
H1-CM1-CM2-CT	27.8400	27.8400	0.0000	0.0000
FCM-CM1-CM2-HC	27.8400	27.8400	0.0000	0.0000
FCM-CM1-CM2-CT	27.8400	-27.8400	0.0000	0.0000
FCT-CT-CM2-HC	0.7450	2.2350	0.0000	-2.9800
FCT-CT-CM2-CM1	0.5951	-1.7853	0.0000	2.3804

^a Parameters a_4 to a_8 are null.

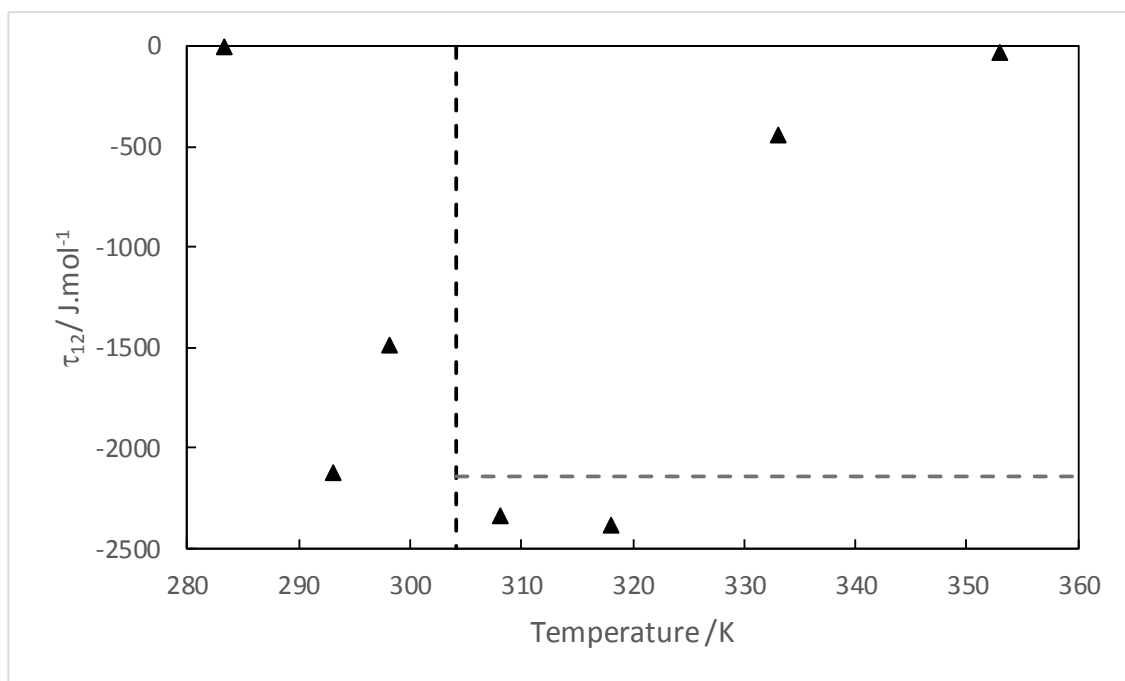


Figure S1: τ_{12} binary parameter as a function of temperature. Vertical dashed: CO_2 critical temperature. Horizontal dashed line: parameter value obtained after considering all the data for $T > T_c(\text{CO}_2)$.

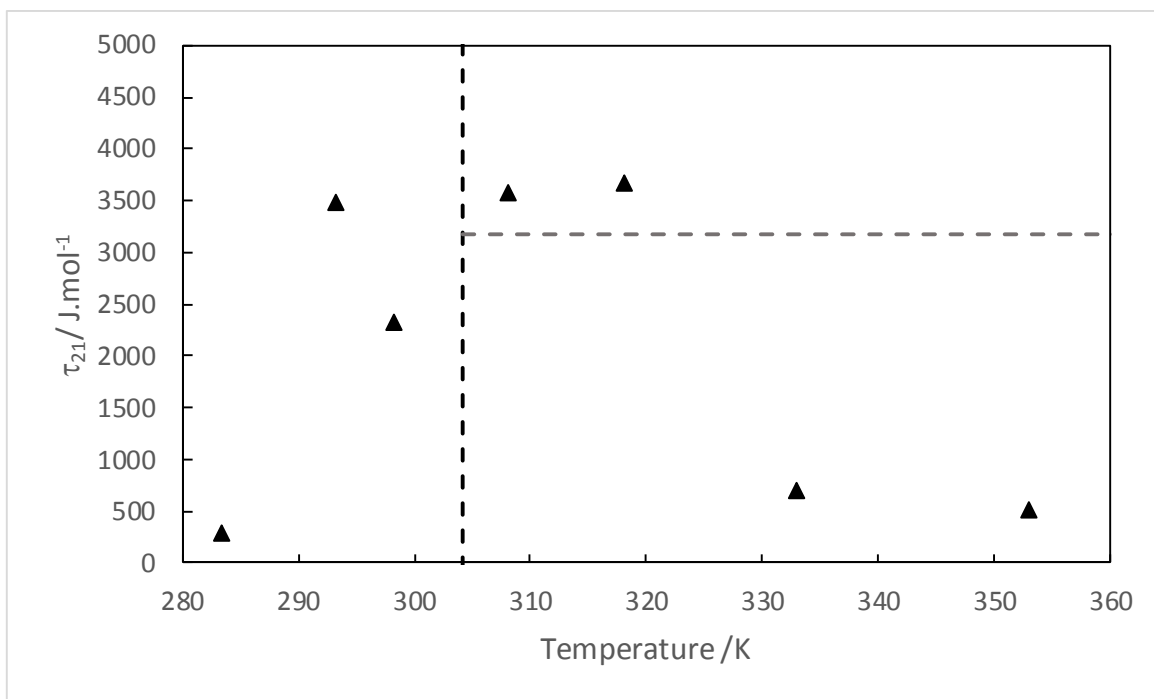


Figure S2: τ_{21} binary parameter as a function of temperature. Vertical dashed line: CO_2 critical temperature. Horizontal dashed line: parameter value obtained after considering all the data for $T > T_c(\text{CO}_2)$.

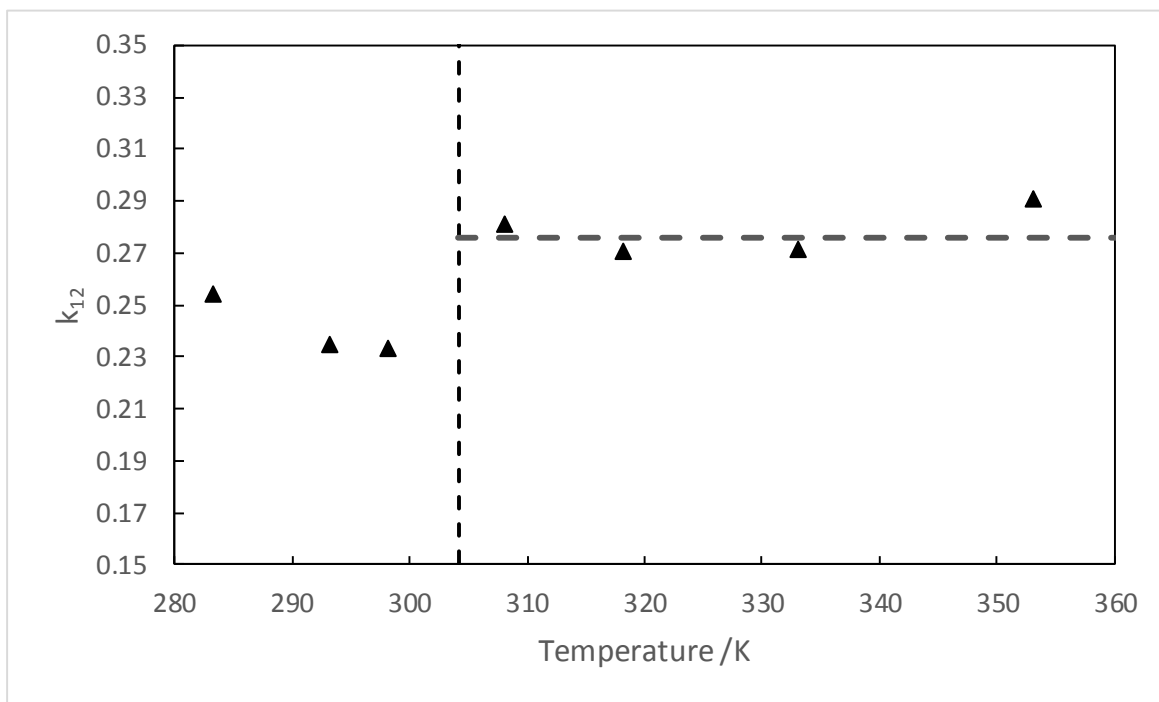


Figure S3: k_{12} binary parameter as a function of temperature. Vertical dashed line: CO₂ critical temperature. Horizontal dashed line: parameter value obtained after considering all the data for $T > T_c(\text{CO}_2)$.

REFERENCES

- [1] J. J. Potoff and J. I. Siepmann, "Vapor-liquid equilibria of mixtures containing alkanes, carbon dioxide, and nitrogen," *AIChE journal*, vol. 47, no. 7, pp. 1676-1682, 2001.
- [2] G. Raabe, "Molecular simulation studies on the vapor-liquid phase equilibria of binary mixtures of R-1234yf and R-1234ze (E) with R-32 and CO₂," *Journal of Chemical & Engineering Data*, vol. 58, no. 6, pp. 1867-1873, 2013.
- [3] E. W. Lemmon, I. Bell, M. L. Huber and M. O. McLinden, *NIST Standard Reference Database 23: Reference Fluid Thermodynamic and Transport Properties-REFPROP, Version 10.0*, National Institute of Standards and Technology, 2018.